

FAULTS/FRACTURES CHARACTERIZATION TO IMPROVE WELL PLANNING AND REDUCE DRILLING RISKS - A CASE STUDY FROM A TIGHT CARBONATE RESERVOIR IN PAKISTAN

MARYAM TALIB, MUHAMMAD ZAHID AFZAL DURRANI,
GHULAM SUBHANI, BAKHTAWER SAROSH and SYED ATIF RAHMAN

Pakistan Petroleum Limited (PPL), 3rd floor, PIDC House, Dr. Ziauddin Ahmed Road, Karachi, Pakistan.

*t_maryam@piol.ae; m_durrani@ppl.com.pk; g_subhani@ppl.com.pk;
s_bakhtawer@ppl.com.pk; r_syed@ppl.com.pk*

(Received February 8, 2022; revised version accepted December 20, 2022)

ABSTRACT

Talib, M., Durrani, M.Z.A., Subhani, G., Sarosh, B. and Rahman, S.A., 2023. Faults/fractures characterization to improve well planning and reduce drilling risks - A case study from a tight carbonate reservoir in Pakistan. *Journal of Seismic Exploration*, 32: 21-38.

Fracture characterization in tight carbonate reservoirs in terms of fracture's relative geometries, orientation, density, and the probability of occurrence has become very important in the exploration and development phase. The future field development plans and production operations in carbonate reservoirs entirely depend on accurate characterization and prediction of the faults and fractures information. In this paper, we synergistically integrated post-stack 3D seismic data, geological background, and drilling history to successfully develop a faults/fractures model of the tight carbonate field in terms of their intensity and direction/orientation information. The workflow involved the removal of the coherent and random noise from the seismic data, calculation of dip compensated edge detection attribute, and improvement in fault/fractures imaging with an advanced automated fault extraction (AFE) algorithm. Finally, discontinuity attributes are used to automatically extract faults/fractures planes information. Markers interpreted from the borehole formation micro-imaging (FMI) helped to calibrate the faults/fractures presence. The studied reservoir consists of Eocene and Paleocene fractured tight carbonate reservoirs in Potwar Basin, onshore Pakistan. The post-stack faults/fractures characterization results proved to be consistent with the geology of the area and validated with the wells data, and the 3D model helped to accurately predict the "sweet spot" within the reservoirs for future drilling of exploration or appraisal wells and improve drilling success.

KEY WORDS: carbonate reservoir, fracture characterization, faults/fracture imaging, edge detection attribute, micro-imaging logs.

INTRODUCTION

Carbonate reservoirs account for more than 60% of the world's oil reserves and are considered the major source of hydrocarbons. Since carbonate reservoirs host a major proportion of petroleum resources, it is very important to properly understand them to effectively find, interpret and characterize them. Usually, these reservoirs are no more difficult than the clastic reservoirs, rather show diversity in the reservoir stratigraphy, diagenesis and rock fabric which significantly influence their ultimate recovery and field development cost. Understanding the diverse nature present in the carbonate depositional system is the key aspect of locating and describing reservoirs characteristic during exploration and field development phases.

Mostly, carbonate reservoirs are naturally fractured and/or have an extensive and extremely complex reservoir settings due to their complicated pore structure and low matrix permeability within small sections of a reservoir (Duan et al. 2021; Josh and Singh 2020; Roehl and Choquette. 1985). Because of their multifaceted tectonics settings, deep burial depth, intricate lithological variations and complex diagenesis complicate both reservoir evaluation, and hydrocarbon recovery (Yasin et al., 2021; Espejel et al., 2020). This requires a proper characterization of the fractal characteristics to understand reservoir heterogeneity, assess the interconnections of the reservoirs, and optimize well locations by understanding the fault/fracture systems in the reservoir (Ding et al., 2020; Wennberg et al., 2016; Nasserli et al., 2015; Boro et al., 2014). Moreover, accurate prediction of fracture systems asserts a considerable impact on the magnitude and direction of fluid flow which consequently affects hydrocarbon (e.g., oil and gas) production (Bear et al., 2012; Berkowitz, 2002; Bonnet et al., 2001; de Dreuzy et al., 2012; Olson et al., 2009). Hence, a primitive understanding of faults/fractures systems and their influence on reservoir characterization, drilling, production, and injection performance pose major challenging tasks for geoscientists (George et al., 2012). However, geoscientists exploited various types of data sets (e.g., seismic attributes, wells logs, drilling cores, and outcrops) to describe the fracture networks based on structural geometry (Deng et al., 2015; Spence et al., 2014; Hunt et al., 2010; Chopra and Marfurt, 2007; Lisle, 1994; Murray, 1968). Faults/fractures are typically imaged as planar discontinuities in the reservoir rock that occur due to the deformation or physical diagenesis and are manually interpreted through visual identification of those discontinuities in the seismic data. Since the early to mid-1990, geoscientists used a variety of seismic attributes such as detection imaging seismic attributes to enhance faults/and fractures visualization and detection (Bahorich and Farmer, 1995). Several geometric seismic attributes based on the edge-detection methods have been successfully applied to delineate faults and fractures such as dip magnitude and azimuth, coherency, semblance, or reflection curvature from seismic reflection data (Al-Dossary and Marfurt, 2006; Hart et al., 2002; Roberts, 2001; Gresztenkorn and Marfurt, 1999; Marfurt et al., 1998; Bahorich and Farmer, 1995). Application of each of these attributes based on their algorithm and workflow provided different information (e.g., coherence, dip and azimuth,

semblance, curvature, and flexure) from seismic data to enhance our capability and to help improve the resolution on fracture characterization and prediction. Consequently, the investigation of carbonate reservoirs requires a careful plan of execution to optimize the intersection of faults or fracture sets. Recent advances and improvements in imaging and automatic faults extraction have provided interpreters with opportunity to automatically interpret faults and fractures, a task traditionally considered to be the most tedious, challenging and time-consuming activity in 3D seismic interpretation to produce automated faults/and fractures models from 3D seismic data (Basir et al., 2013; Pedersen et al., 2001; Randen et al., 2000; Crawford and Medwedeff, 1999; Dorn and James, 2005; AlbinHassan and Marfurt, 2003).

This paper focuses on extracting fractures (fracture corridors) in terms of intensity/magnitude, direction/orientation, and density information from migrated post-stack 3D seismic data volume. We employed advanced faults/and fractures characterization and interpretation workflow introduced by Dorn et al. (2012) to extract faults/fractures density attribute and their orientations with enough accuracy and continuity in tight fractured carbonates reservoir from post-stack 3D seismic data. The workflow consists of seismic data quality check and conditioning (removal of noise), calculation of dip compensated edge detection attribute, and improvement in fault/fracture imaging by generating fracture probability volume from the automated fault enhancement (AFE) algorithm. Very often, seismic attributes are sensitive to noise and it necessitates further treatment for noise reduction and improvement in the seismic data quality before computing the attributes. Therefore, input seismic amplitude data is conditioned through dip-guided coherent and random noise removal processes. Based on the seismic amplitude variation, the edge detection attribute (i.e., horizon edge stack attribute) is computed which is further enhanced through the automated fault enhancement (AFE) algorithm. The outputs of AFE are used as input for the automated fault extraction process and planar clustering. Finally, validation, calibration, and interpretation of the extracted faults/fractures are performed based on available well information (formation micro-imaging logs) and the geological knowledge relating to the existence of faults/fractures in the region. For further analysis of results, rose diagrams from the drilled wells were used to highlight extracted fracture planes striking along the specific directions. The post-stack faults/fractures characterization results are found to be consistent with the geology of the area and validate with the wells' data (e.g., FMI logs) information. The example of the results of applying the processes and workflow is presented to test Eocene (Chorgali/Sakessar) and Paleocene (Patala/Lockhart) carbonate plays from a newly discovered oil field lying in the Potwar Basin, onshore Pakistan. Potwar basin is one of the major hydrocarbons producing tertiary basins in Pakistan. The complexity of the geological structure in this area provides a challenging environment to properly characterize faults/fractures to improve the well drilling process and optimize the well planning strategy for field development. Detecting and understanding the presence of faults/fractures and their continuity in the field is crucial to help build the strategy in drilling and well path planning.

The presence of faults/fractures and their continuity in the target interval and the challenges encountered during the drilling process in the drilled wells are the major concerns that need to be detected before the drilling.

BACKGROUND GEOLOGY

The study area lies at the western margin of the Potwar Plateau which is a part of the active foreland fold and thrust belt of the Himalayas in Northern Pakistan (Burbank and Reynolds, 1988; Jaumé and Lillie, 1988; Pennock et al., 1989) (Fig. 1a). The geological history of the region is complex and is marked by several unconformities. The region observed large marine, and at times terrestrial environments from the Precambrian to recent. Major fold - Jhamat anticline comprising the exploration target marks the East-West trending major surface feature passing through the northern part of the block which is bounded by the Chab syncline in the south and Girdi syncline in the north. These two major synclines are considered to be the main kitchen areas and fed the hydrocarbons to the adjacent structures. In terms of petroleum systems, the hydrocarbon source comes from Patala shales of Paleocene and intraformational shales within the Nammal formation (Eocene) which is considered the most prolific source rock units of the Potwar Basin. The reservoirs targeted in the area include Chorgali and Sakesar Limestone of Eocene and Patala and Lockhart Limestone of Paleocene age and the hydrocarbon production from limestones is mainly dependent upon the development of fracture porosity (Fig. 1b).

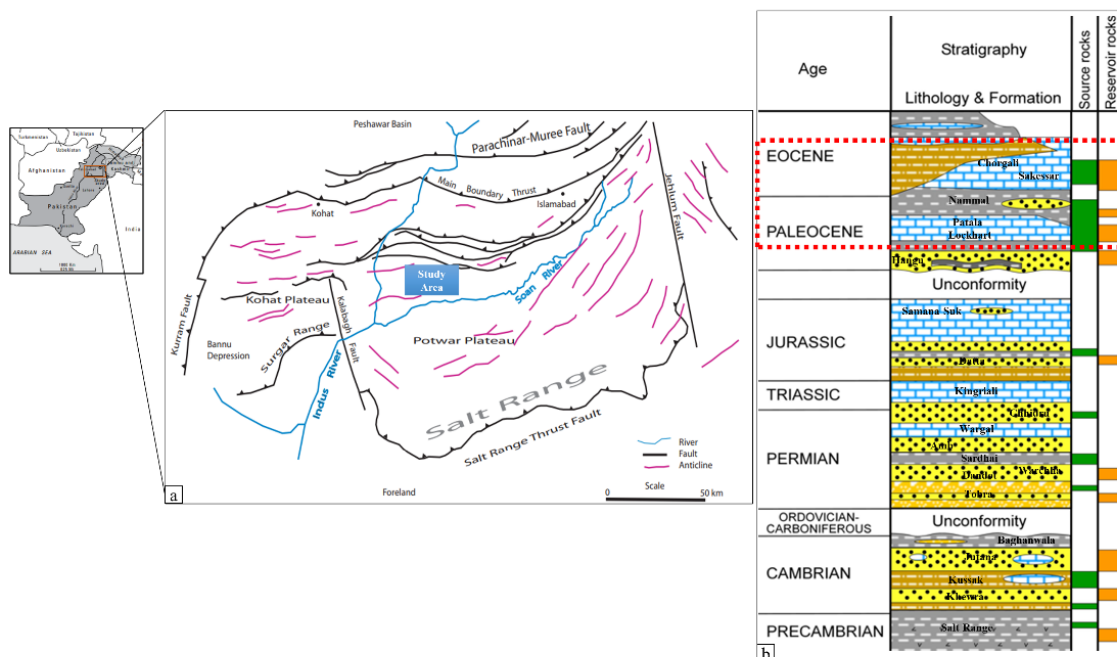


Fig. 1. Geological setting; (a) structural map of the Kohat-Potwar Plateau, onshore Pakistan (study area highlighted in blue) and (b) stratigraphy column of the area (target interval highlighted in blue) (Wandrey et al., 2004).

The 3D seismic data is acquired over the field to delineate the subsurface structural geometry and extent of the drilled structure. Seismic data interpretation reveals that the structure consists of three compartments and all these compartments are separated by major east-west trending thrust faults. Fig. 2a shows the depth structural map at the top of the Paleocene reservoir formation, depicting three structural compartments bounded by the East-West trending major faults. The analogue conceptual model of the expected fractures represents fracture (continuous/discontinuous) patterns on a thrust-related folded stratum from an excessively deformed complex geology of the tight (low porosity) carbonate reservoir (Fig. 2b). Different fractures sets are expected on the thrust-related folded strata and their orientation relates to the fold geometry and regional thrust transport direction.

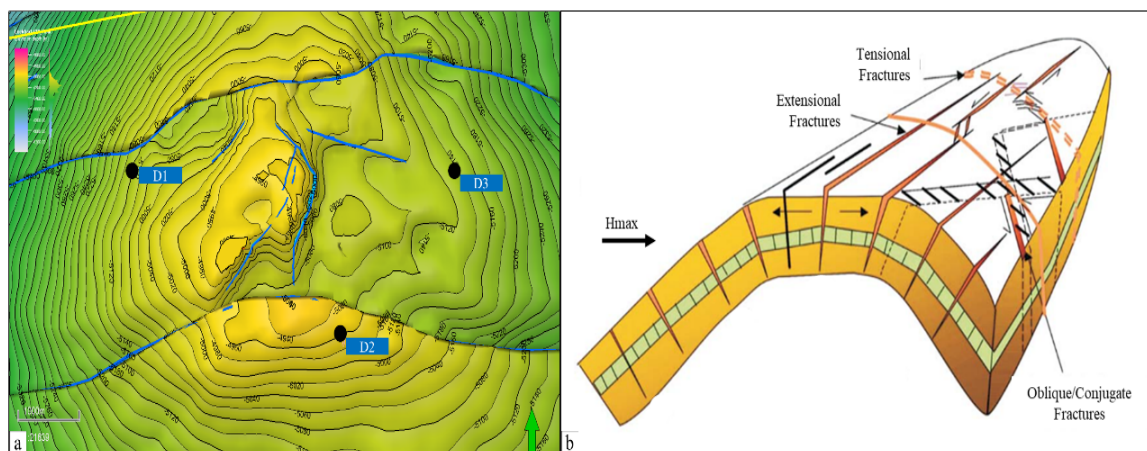


Fig. 2. (a) Depth structure map at the reservoir target (Paleocene formation) clearly showing three compartments separated by major east-west trending faults along with drilled well's location in those compartments; (b) Conceptual model of the expected fractures characteristics on a thrust-related folded stratum (modified from Jadoon et al., 2007).

Available Data

To achieve the objectives of the study, following dataset have been used:

- i) *3D scaled seismic data processed using Reverse Time Migration (RTM) which served as an input for the study.*
- ii) *Interpreted horizons to analyse the results on target intervals.*
- iii) *Well information from two wells such as FMI/Sonic Scanner data for QC and validation of the results.*

All the above datasets have been subjected to standard quality check and appropriate conditioning processes have been applied to prepare the data for post-stack faults/fractures characterization workflow.

METHODOLOGY/WORKFLOW

We have employed a faults/fractures identification workflow which is quite advanced compared to traditional methodologies which simply rely on the seismic multi-attributes (e.g., coherency, curvature, etc.). Fig. 3 shows the schematic of the employed workflow which involves; i) removal of the coherent and random noise from the input post-stack 3D seismic data volume using unique structurally oriented filters, ii) calculating a tunable edge detection attribute with dip guidance, iii) faults/fractures enhancement using Advanced Fault Enhancement (AFE) algorithm, iv) extraction and organization of fault surfaces through planar clustering, and v) calibration of results using well control.

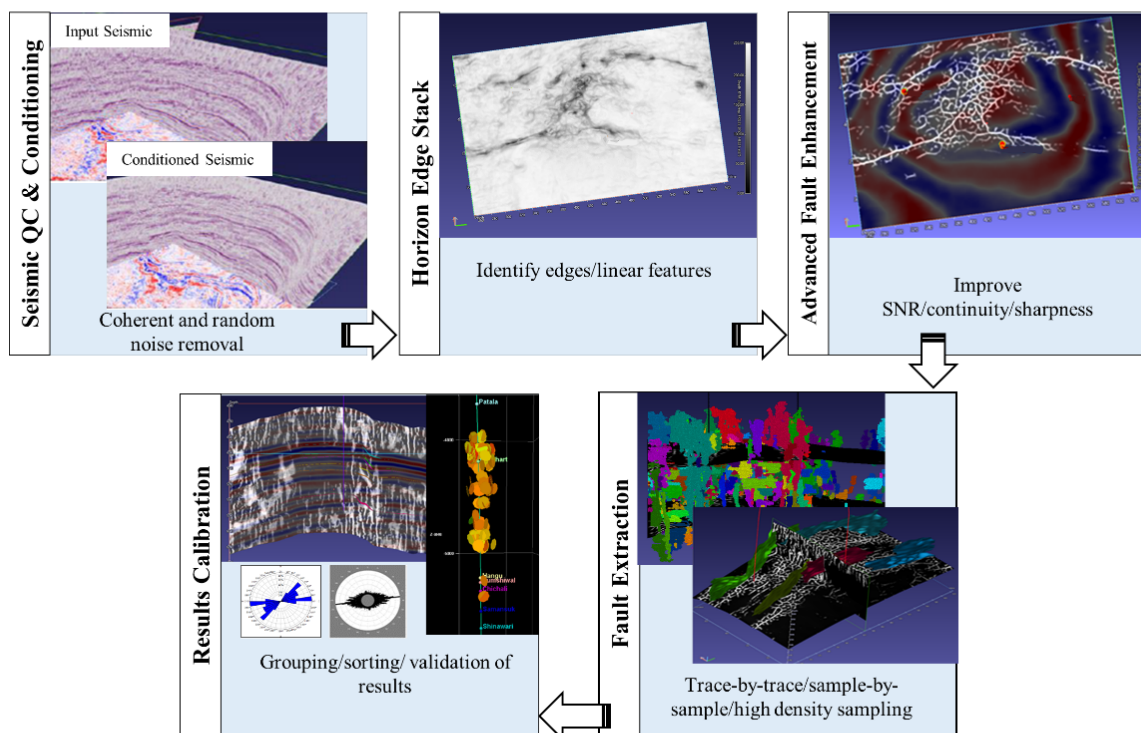


Fig. 3. Fault/fracture characterization workflow for 3D post-stack seismic data adopted for the study (modified after Dorn et al., 2012).

Seismic data QC and conditioning is considered as the elementary step of the workflow to highlight subtle but potentially important structural and stratigraphic features by enhancing seismic events continuity and removing inherent noises. The input seismic stack data quality has been checked for the presence of noises and several data conditioning processes have been applied during the workflow to remove the noise and enhance the signal. Two types of filters are used for this purpose; i) coherent noise removal to eliminate acquisition footprint artefacts (e.g., stripping) and ii) random noise removal based on statistical filtering to further smoothen the seismic volume. Quality control (QC) of each process is performed by

analyzing the amplitude residuals before and after the application of each process. For seismic edge detection, the horizon edge stack (HES) attribute is extracted which identified edges and discontinuities from the input-conditioned seismic amplitude and horizon orientation (HO) volume for the dip guidance. It uses a cross-shaped operator to calculate the amplitude change in inline and crossline direction by running the operator for every sample position along the depth axis. This calculated HES attribute relates to geological discontinuities/lineament in the coherent seismic reflectors and pictured on the horizon edge stack as faults/fractures.

The advanced fault enhancement (AFE) algorithm further enhances steeply dipping planar features from structurally oriented horizon edge stack by using multiple windowed radon transforms which improved the imaging of identified faults. The radon-transform computes the projection of an image matrix along specified directions, i.e., strike, dip, and fault plane from the HES volume. The process is performed stage by stage as per specified direction. The result can be thought of as a faults/fractures probability volume with high values indicating a high probability of fault presence. These accurate (trace-by-trace and very high-density sampling) images of faults/fractures provide improved resolution and signal strength in the output fault/fracture probability volume which are further used for auto-extraction of 3D fault planes.

Initially, fault cuts are generated based on the voxel value on the depth slices from the input volume. This process does not consider vertical connectivity; considers only lateral connectivity and therefore does not produce connected 3D planar objects. This allowed us to further filter remaining noise and extract the faults of certain ranges. The finalized fault cuts are then used as seeds for the subsequent planar clustering to generate 3D connected planar features. For further analysis of results, rose diagrams are used to re-cluster fault segments striking along specific directions. To analyze and interpret the results, well data such as image logs (e.g., FMI) and drilling events are integrated to calibrate direct information about subsurface rock conditions which helped to confirm if the extracted faults/fractures from seismic have intersected the well. The processes in the workflow are seamlessly integrated to quickly identify and accurately interpret faults/fractures in complicated structural environments and locate areas of enhanced fracturing and identify sweet spots for optimal well placements.

RESULTS ANALYSIS and DISCUSSION

In this case study, we have applied the proposed faults and fractures imaging workflow on 3D post-stack seismic (RTM) data in a stepwise framework to characterize Eocene and Paleocene carbonate reservoirs in Potwar Basin. The results and their discussion of each step are presented in the relevant sub-section headings below.

Seismic Data Conditioning

Seismic data conditioning is the first step of data processing to ensure the best possible results. Before performing seismic data conditioning, the original scaled RTM seismic data is cropped to stay focused over the targeted objective window covering Eocene and Paleocene reservoirs. Two types of filtering are applied in this phase to remove inherent noises namely coherent and random noises. To remove coherent noise, the filtering process is performed iteratively by using a different set of parameters. Removal of coherent noise artifacts early in the workflow has the benefit of yielding superior input for subsequent steps in the workflow by providing high-quality and authentic seismic reflections which are important for workflows that seek to enhance linear features. Random noise filtering used here is based on a statistical filter that smoothens the input volume using one of the varieties of smoothing algorithms (e.g., such as mean, median, mode, alpha-trimmed mean, and symmetric nearest neighbor). In this study, a median filter is used with the parameters defining the size of the smoothing operator. To QC the effect of noise removal, seismic amplitudes, and residuals are compared before and after the application of each process. Fig. 4 shows the comparison of seismic data before and after conditioning with the amplitude residuals showing the coherent and random noise features only that have been removed from the seismic improving the quality of seismic amplitudes.

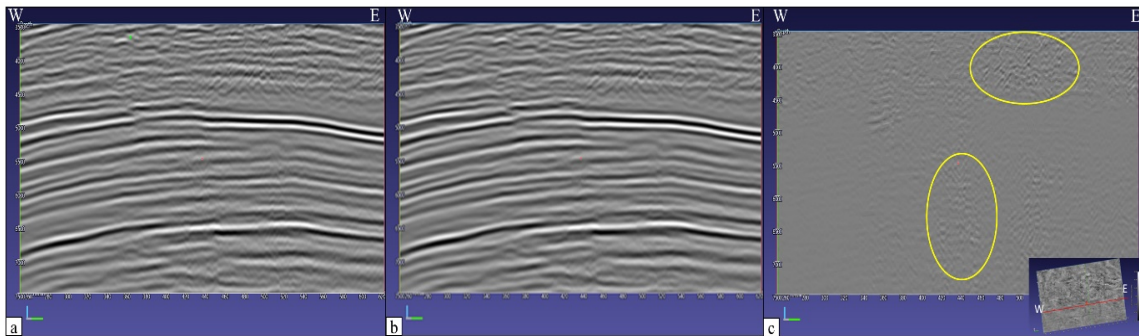


Fig. 4. Seismic data conditioning; (a) before conditioning input seismic, (b) conditioned seismic after removal of coherent and random noise, and (c) residuals showing the noise only (highlighted in yellow).

Horizon Edge Stack (HES) Attribute

Horizon edge stacking (HES) is a coherence class attribute that illuminates subsurface geomorphology and identifies correlated geological discontinuous features in the seismic reflections. This attribute can also be used to identify the non-geological artifacts (such as coherent noise), an essential process in the workflow because of its propensity to severe sensitivity to the noise. Due to the onshore nature of the seismic data, the noise removal process is applied in various orientations to encounter the footprints affect in the data which comprise of multiple wavelengths.

The HES employs sample-by-sample amplitude change computation in seismic data along the inline and crossline directions and repeats the cross-shaped operator calculations for every sample positioning along the “z” axis defined by the user’s choice of “stack length” parameter. HES used input noise-filtered conditioned seismic amplitude volume guided by horizon orientation (HO) volume for initial fracture mapping. The HO process calculates the orientation of horizons in the input seismic volume using the Gradient Structure Tensor (GST) yielding a three-component vector volume that provides both strike and dip of data. Fig. 5 shows the dip and strike extracted for the area under study depicting close to vertical major faults.

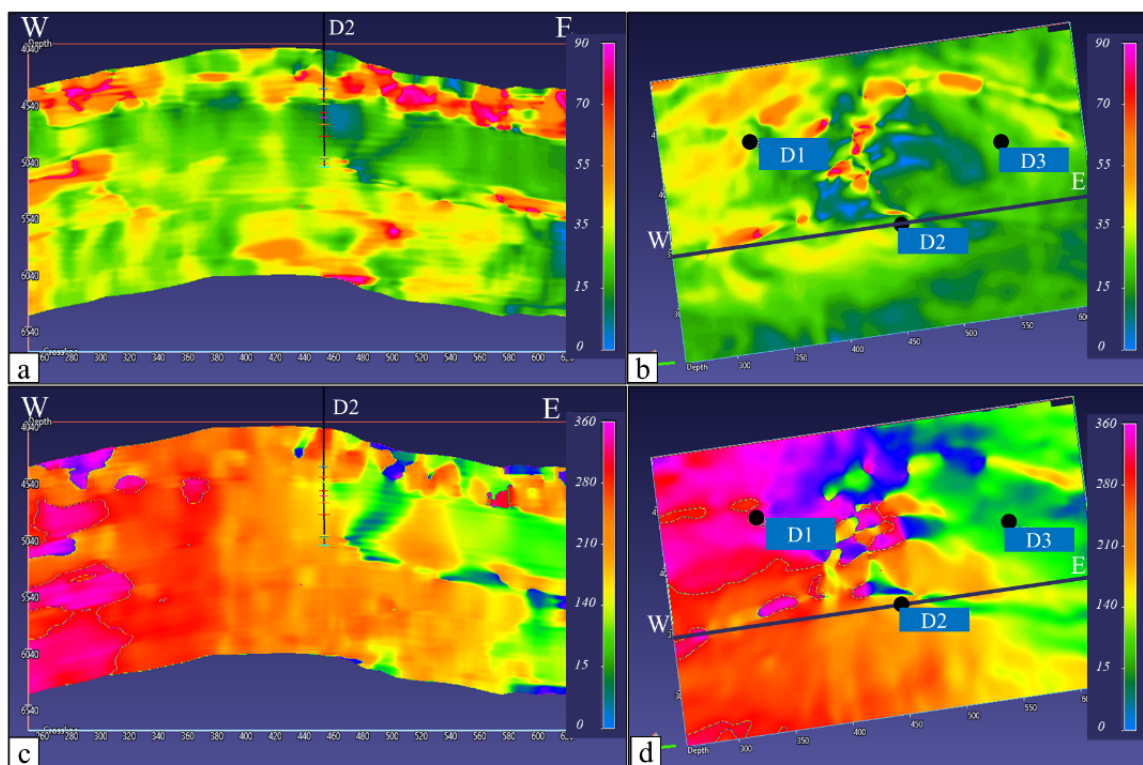


Fig. 5. Horizon orientation for dip guided application of HES attribute; (a) and (b) Dip W-E cross-section and map at the target interval (5150mSS) showing near vertical ($\sim 90^\circ$ dip) major thrust faults, (c) and (d) Strike W-E cross-section and map at the target interval (5150mSS)

Assigning a HO volume to the input allows the HES process to be directionally applied using X, Y and Z vector information. Depth diameter and horizon attenuation are used as controlling parameters to generate an optimum HES attribute. Fig. 6 shows the cross-section and map view of HES volume which indicates faulted and fractured areas in the field.

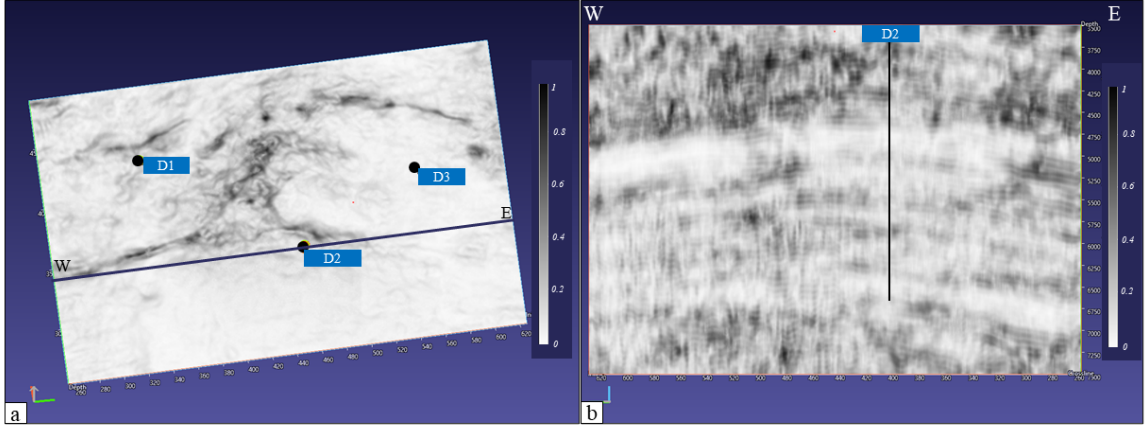


Fig. 6. Horizon edge stack attribute; (a) map view at target interval (5150mSS) with white color showing the continuity of seismic reflections and black color depicting the discontinuities/edges and (b) W-E cross-section passing through D2 well location.

Advanced Fault Enhancement (AFE)

The advanced fault enhancement (AFE) imaging algorithm uses windowed Radon transforms. Practically, the windowed Radon transform is applied in three key steps:

1. Fault orientations are imaged in the edge detection attributes volumes (volume),
2. Supporting geological fact that faults are locally a dipping planar surface, and
3. Using fault strike and dip to orient the AFE processes.

In this case study AFE process is performed stepwise with strike enhancement as the first stage by using HES attribute as an input for initial imaging of faults on horizontal (time/depth) slices. Windowed radon-transform oriented horizontally is applied at each point on the edge attribute volume to yield strike enhanced (SE) output volume and strike orientation (SO) volume. The SE value at a point in the volume represents the probability of a horizontal lineament passing through that sample and SO value represents the strike of that lineament. Mathematically, SE can be defined by the following equation (Dorn, 2019):

The Strike Enhance (SE) attribute is computed at each sample point in the edge attribute volume predominantly on a horizontal sli

$$SE(x, y, z) = \max_{\sigma=0.180} \left[\int_{-a}^a (HES(\sigma, r)/2a) dr \right] , \quad (1)$$

$$S = \sigma_{max} . \quad (2)$$

Dip enhancement (DE) uses the previous output from SE stage as input to estimate SE volume at each sample point particularly on the vertical

slice oriented perpendicular to strike (S) volume. With the strike (S) value calculated at each sample in the volume, the second radon transform is applied on vertical slices of the SE volume, where each vertical slice is oriented perpendicular to strike orientation (i.e., azimuthal direction of local fault dip). This produced a volume of dip enhanced (DE) and dip values which represent 2D vector dip in a direction that is perpendicular to strike in the volume, which can be described as follows:

$$DE(x, y, z) = \max_{\delta=0.90} \left[\int_{-b}^b (SE(\delta, r)/2b) dr \right] , \quad (3)$$

$$D = \delta_{max} . \quad (4)$$

The DE , strike and dip volumes contain enough information to orient a small planar surface to estimate fault dip at each sample in the DE volume to honour the geologic requirement of local planarity for a fault.

The final step in the process integrates the DE values on dipping circular planes centred on each sample in the volume. This step also refined the estimate of the 3D dip vector at each point. The output from this final stage of the process is the fault enhanced (FE) volume representing the probability of a dipping planar feature passing through each sample, and a final fault orientation volume which is comprised of the x , y , and z components of the 3D fault dip vector at each sample in the volume. FE at each sample point in the DE volume, on the dipping plane defined by:

$$FE(x, y, z) = \int_0^{180} \int_{-c}^c (DE(\phi, c, r)/2c) dr d\phi , \quad (5)$$

$$FO = (\phi_x, \phi_y, \phi_z) , \quad (6)$$

where:

HES = Horizontal Edge Stack attribute value at a point in the volume

SE = Strike enhanced attribute value at each point in the volume

S = Strike of the ES discontinuity

DE = Dip enhanced attribute value a point in the volume

D = Dip of the SE discontinuity

FE = Fault enhanced (3D fault probability scaled between 0 and 1) at each point in the volume.

FO = Fault orientation (x , y , and z components of 3D vector dip) at each point in the volume.

(x, y, z) = Co-ordinates of the sample in the volume where the calculation in being applied.

σ = Dip on the horizontal plane (time/depth slice) relative to North.

δ = Dip on the vertical plane oriented perpendicular to strike.

ϕ = 3D dip vector

a = Radius (r) in samples of the windowed Radon transform operator on a horizontal slice.

b = Radius (r) in samples of the windowed Radon transform operator on a vertical slice oriented perpendicular to S .

c = Radius (r) of the operator on the dipping plane defined by strike and dip.

The objective of the each of the step involved in the workflow improves the imaging of the faults while eliminating the undesired background noise.

Fig. 7 shows the improvement of faults/fractures imaging after SE, DE, and FE volumes computations overlaid with seismic amplitude volume.

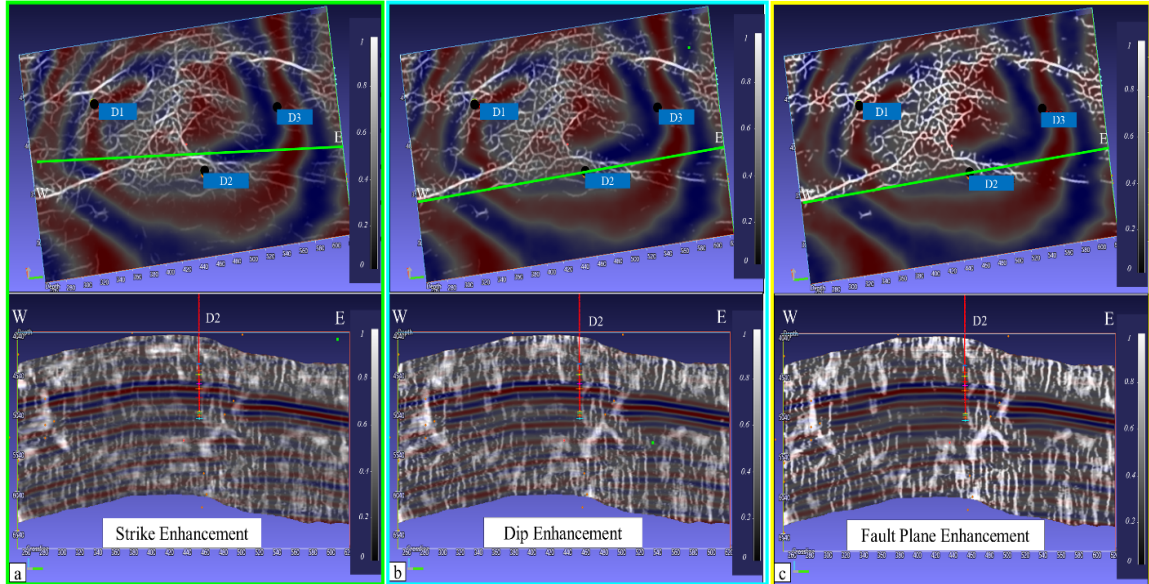


Fig. 7. Advance fault enhancement (AFE); (a) strike enhancement, (b) dip enhancement, and (c) fault plane enhancement. Map at target interval (5150mSS) and W-E cross-section passing through D2 well location of AFE co-rendered with seismic amplitudes showing the higher probability of faults/fractures presence (in white color) and the improvement of faults/fracture imaging with strike, dip, and fault plane enhancement, respectively.

Fig. 8 shows the strike and dip volumes extracted for each dipping planar feature in comparison with the geometric seismic attribute curvature which is used to compare faults and fractures prediction. However, the AFE attribute provides a more robust set of fractures and faults prediction when compared with the curvature attribute. The curvature attribute fails to completely capture the extent of the fault/fracture as well as fracture density highlighted in (Figs. 8b and 8c). However, the AFE attribute properly captures the fault and fracture extent and fracture density at well D1 which is calibrated through well data.

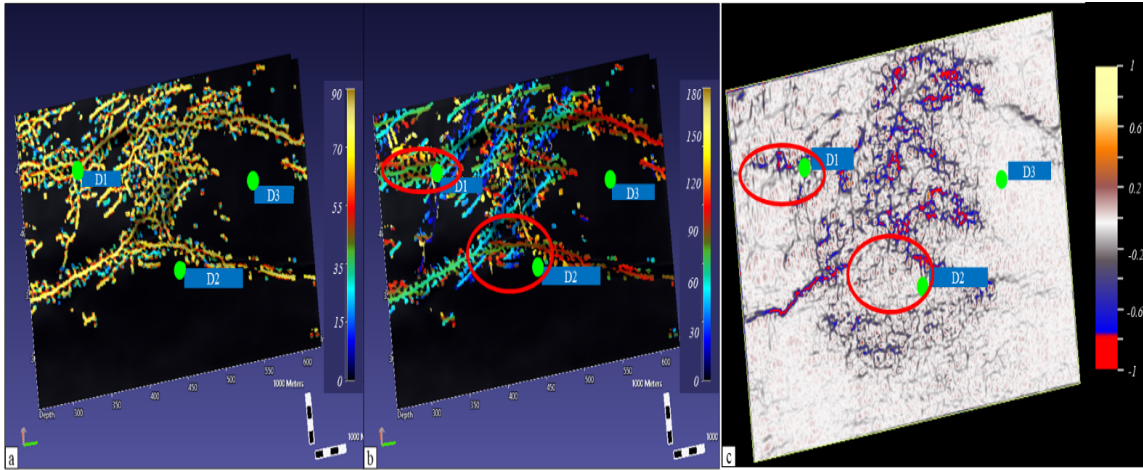


Fig. 8. Probable faults/fractures orientation; (a) Map of probable faults/fractures dip at the target interval (5150mSS) showing the dip of major thrust fault at 90° , (b) map of probable faults/fractures strike at the target interval (5150mSS), and (c) curvature attribute showing fault/fracture at the target interval (5150mSS).

FAULT CUTS EXTRACTION AND PLANAR CLUSTERING

Through an automated fault extraction process, we generated the fault cut lineaments that approximate the location of faults in the seismic volume using fault enhanced and fault orientation volumes as input. This process generated the fault cuts on depth slices based on the voxel value in the input volume. There are two parameters in this process namely minimum fault cut length and minimum voxel value that are customized based on the objective. The minimum fault cut length sets the minimum number of adjacent samples to be equal to or greater than the minimum voxel value to begin drawing an extracted fault cut on any given time/depth slice. The minimum voxel value is the minimum value in the fault-enhanced volume that will be considered in the process of placing seeds to generate fault planes. These fault cuts are then used as seeds for the subsequent planar clustering process. Planar clustering took the fault cuts as an input set of points and regrouped the points into 3D connected planar features. The planar clustering parameters control how planar a feature must be as well as its minimum accepted size. The advanced parameters allow fine-tuning of the tolerances. The parameters used in this process are cluster size and coplanarity constraints. Cluster size determines the minimum size (number of points) for outputting a clustered object (such as small, default, large, very large, etc.). Coplanarity constraints select what conditions are applied to define co-planar groups of points such as conservative, default, or liberal. Fig. 9 displays the unrestricted extracted faults/fracture planes through the planar clustering process at the target intervals which are further re-grouped based on the geological knowledge and interpretation of well information through the rose diagram.

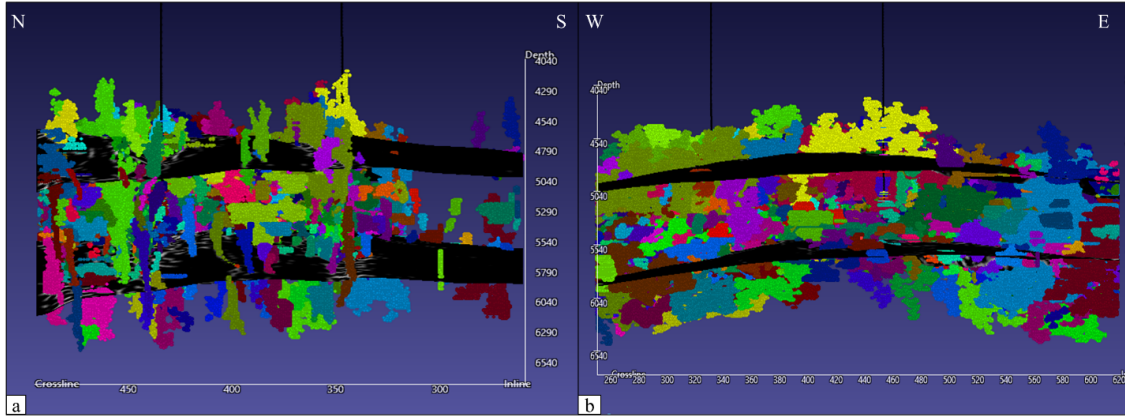


Fig. 9. Extracted fault/fracture planes through Planar Clustering; (a) inline view (N-S cross-section) of extracted fault/fracture planes within the target interval (Eocene & Paleocene carbonates) with each fault/fracture plane highlighted in different color and (b) crossline view (W-E cross-section) of extracted fault/fracture planes.

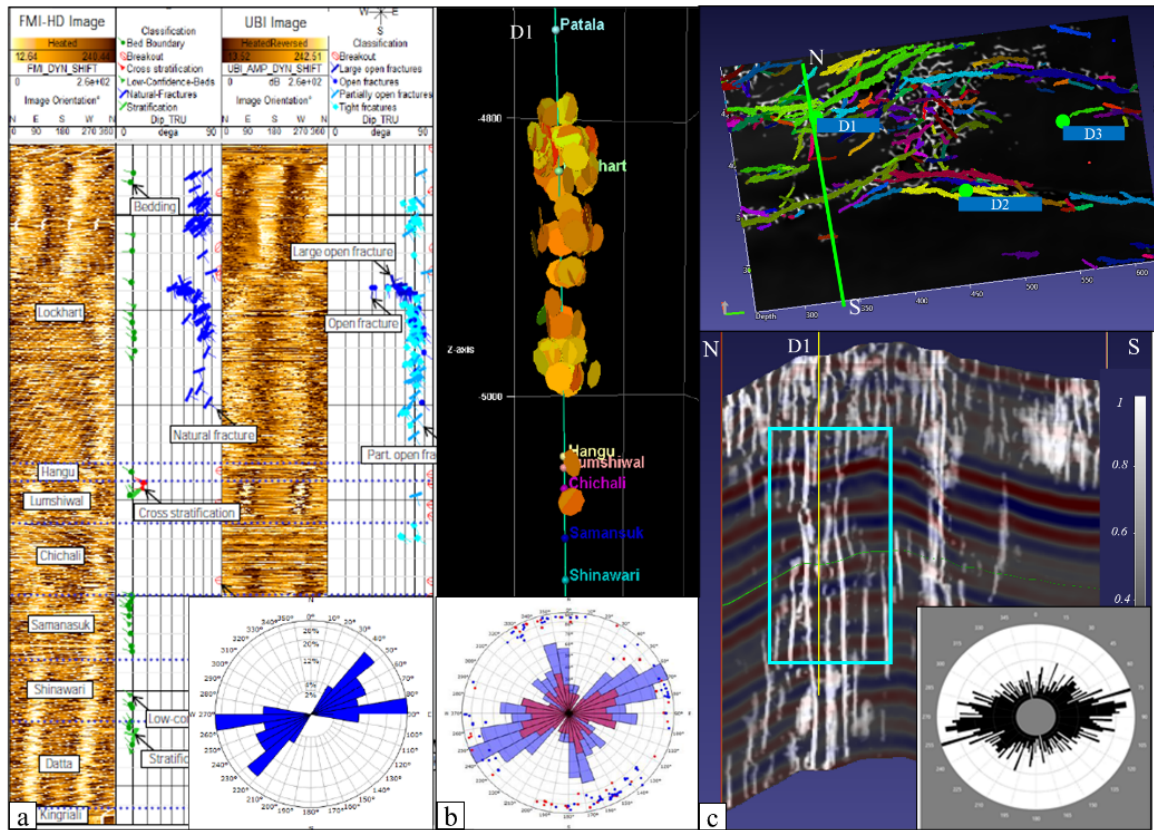


Fig. 10. Calibration of faults/fractures extracted from seismic with the FMI/UBI and 3D far-field sonic scanner data (FFS); (a) FMI/UBI data from D1 along with the strike rosette of open fractures showing near vertical dip and NE-SW strike of fractures, (b) features captured from 3D FFS (monopole & dipole) with the strike rosette (X dipole in red and Y dipole in blue) showing major NE-SW direction with some features in the opposite direction, and (c) Map view of extracted faults/fractures from seismic within the target interval (Eocene & Paleocene carbonates) and N-S cross-section along the D1 well showing the presence of faults/fractures (in white) co-rendered with seismic amplitudes along with strike rosette of extracted faults/fracture planes from seismic. Dominant west-east trend with near vertical dip of faults/fractures is clearly captured on seismic data calibrated with FMI/UBI and 3D FFS data.

Analysis and Interpretation of Results

Analysis and interpretation of the results can be carried out in several different ways. The most common method of analysing the results is to compare them with similar information from regional geological knowledge and wells data. Formation micro-imaging (FMI) log, ultrasonic borehole imaging (UBI) log, 3D far-field sonic scanner interpretation results, and drilling experience helped to prove the validity of extracted faults/fractures from seismic. The use of FMI, UBI, and sonic scanner data to corroborate the findings from the present study can be seen in Fig. 10. The strike azimuth is compared between extracted results, and the major trend from well taking some samples from FMI/UBI and sonic scanner. The post-stack based faults/fractures imaging results are consistent with the local geology and wells data showing major East-West (E-W) trending faults.

Besides using strike direction through rose diagram analysis to sort the faults/fractures, the size of extracted faults/fractures is also used to interpret the extracted fault planes. Fig. 11 shows the major fault planes based on the size and the strike direction from the rose diagram analysis depicting the west-east trend which is well captured.

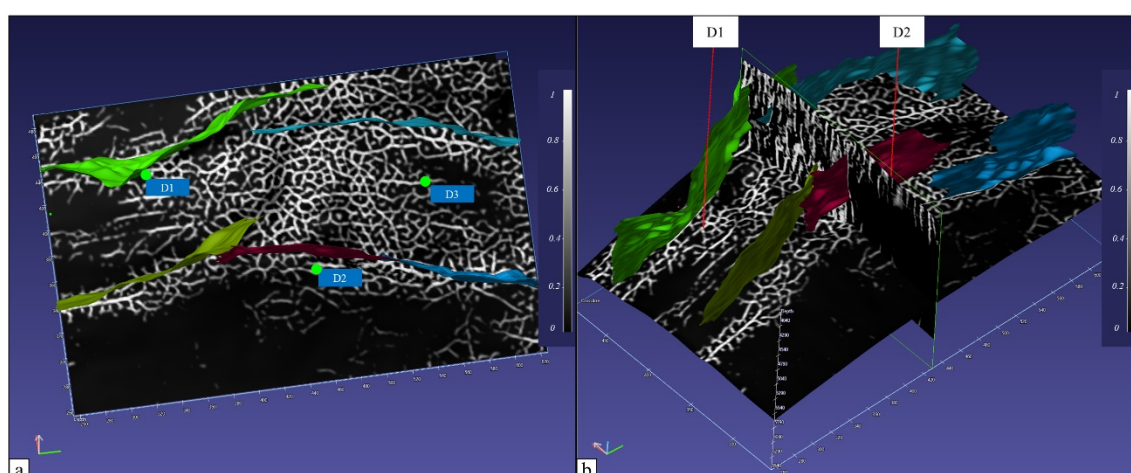


Fig. 11. Sorting of fault/fracture planes based on the size; (a) map of extracted fault/fracture planes with size >10,000 points within target interval (Eocene & Paleocene carbonates) and (b) 3D view of extracted fault/fracture planes showing that only major faults (oriented west-east) are captured with the cut-off of size >10,000 points.

CONCLUSIONS

Post-stack based fault/fracture imaging using advanced automated technology proved to be a valuable aid in characterizing tight fracture carbonate formations (Eocene and Paleocene) from a recently discovered oil field lying in the Potwar basin of Pakistan. Seismic data conditioning improved the quality of seismic amplitudes which proved an imperative step in the noise-sensitive workflows. Parameters are customized for the horizon

edge stacking (HES) and advance fault enhancement (AFE) based on the objective to maintain the continuity of major faults and keeping the fractures at proven intervals from the wells. The fault-enhanced volume indicated the area of faults/fractures whereas the fault orientation volume provided the strike and dip information of extracted faults/fractures. Rose diagrams are used to interpret the major faults trends and to sort based on their strike azimuth. Rose diagram analysis is also compared to the existing well information such as FMI and sonic scanner. The study revealed several faults that are encountered during the drilling of the previous wells and identified areas of enhanced fracturing for future well placement. The faults/fractures extracted from depth migrated post-stack seismic (RTM) data proved to be consistent with the geology of the area showing major East-West trending faults. This result can be used judiciously, in the future, for successful well-planning during the appraisal and field development phases.

ACKNOWLEDGEMENTS

The authors would like to acknowledge Pakistan Petroleum Limited (PPL) management; especially Arshad Palekar [Senior Manager Exploration (North)] and JV partner Government Holding Private Limited (GHPL) for their support and for allowing the publication of this paper. We also would like to extend our appreciation toward Geosoft technical team (Jimmy ting, Rino Saputra, and Reza Becti) for sharing their expertise in the proof-of-concept (POC) study carried out in northern Indus basin of Pakistan.

REFERENCES

- AlBinHassan, N.M. and Marfurt, K.J., 2003. Fault detection using Hough transforms. Expanded Abstr., 73rd Ann. Internat. SEG Mtg., Dallas: 1719-1721.
- Al-Dossary, S. and Marfurt, K.J., 2006. 3D volumetric multispectral estimates of reflector curvature and rotation. *Geophysics*, 71: 41-51.
- Bahorich, M. and Farmer, S., 1995. 3-D seismic discontinuity for faults and stratigraphic features: The coherence cube. *The Leading Edge*, 14: 1053-1058.
- Basir, H.M., Javaherian, A. and Yarak, M.T., 2013. Multi-attribute ant-tracking and neural network for fault detection: a case study of an Iranian oilfield. *J. Geophys. Engineer.*, 10: 015009.
- Bear, J., Tsang, C.F. and De Marsily, G. 2012. *Flow and Contaminant Transport in Fractured Rock*. Academic Press, New York.
- Berkowitz, B., 2002. Characterizing flow and transport in fractured geological media: A review. *Advanc. Water Resour.*, 25(8-12): 861-884.
- Bonnet, E., Bour, O., Odling, N.E., Davy, P., Main, I., Cowie, P. and Berkowitz, B., 2001. Scaling of fracture systems in geological media. *Rev. Geophys.*, 39: 347-383.
- Boro, H., Rosero, E. and Bertotti, G., 2014. Fracture-network analysis of the Latemar Platform (northern Italy): Integrating outcrop studies to constrain the hydraulic properties of fractures in reservoir models. *Petrol. Geosci.*, 20: 79-92.
- Burbank, D.W. and Reynolds, R.G.H., 1988. Stratigraphic keys to the timing of thrusting in terrestrial foreland basins; Applications to the north-western Himalaya. In: Kleinspehn, K.L. and Paola, C., Eds., *New perspectives in basin analysis*. Springer-Verlag, New York: 331-351.

- Chopra, S. and Marfurt, K.J., 2007. Volumetric curvature attributes add value to 3D seismic data interpretation. *The Leading Edge*, 26: 856-867.
- Crawford, M. and Medwedeff, D.A., 1999. Automated extraction of fault surfaces from 3-D seismic prospecting data. U. S. Patent 5,987,388.
- Deng, X.L., Li, J.H., Liu, L. and Ren, K.X., 2015. Advances in the study of fractured reservoir characterization and modelling. *Geol. J. China Univ.*, 21: 306-319.
- Ding, Y., Du, Q., Yasin, Q., Zhang, Q. and Liu, L., 2020. Fracture prediction based on deep learning: Application to a buried hill carbonate reservoir in the S area. *Geophys. Prosp. Petrol.*, 59: 267-275.
- De Dreuzy, J.R., Méheust, Y. and Pichot, G., 2012. Influence of fracture scale heterogeneity on the flow properties of three-dimensional discrete fracture networks (DFN). *J. Geophys. Res., Solid Earth*, 117: B11207.
- Dorn, G.A. and James, H.E., 2005. Automatic fault extraction in 3-D seismic interpretation. *Extended Abstr.*, 67th EAGE Conf., Madrid: F035.
- Dorn, G.A., Kadlec, B. and Murtha, P., 2012. Imaging faults in 3D seismic volumes. *Expanded Abstr.*, 82nd Ann. Internat. SEG Mtg., Las Vegas.
- Dorn, G.A., 2019. 3D fault imaging using windowed Radon transforms: an example from the North Sea. *First Break*, 37(5): 81-88.
- Duan, R., Xu, Z., Dong, Y. and Liu, W., 2021. Characterization and classification of pore structures in deeply buried carbonate rocks based on mono- and multifractal methods. *J. Petrol. Sci. Engineer.*, 203: 108606.
- Espejel, R.L., Alves, T.M. and Blenkinsop, T.G., 2020. Multi-scale fracture network characterisation on carbonate platforms. *J. Struct. Geol.*, 140: 104160.
- George, B.K., Clara, C., Al Mazrooei, S., Manseur, S., Abdou, M., Chong, T.S. and Al Raeesi, M., 2012. Challenges and key learning for developing tight carbonate reservoirs. *Internat. Petrol. Conf. Exhib.*, Abu Dhabi, UAE (SPE- 161693-MS).
- Gresztenkorn, A. and Marfurt, K.J., 1999. Eigen structure-based coherence computations as an aid to 3D structural and stratigraphic mapping. *Geophysics*, 64: 1468-79.
- Hart, B.S., Pearson, R. and Rawling, G.C., 2002. 3D seismic horizon-based approaches to fracture-swarm sweet spot definition in tight-gas reservoirs. *The Leading Edge*, 21: 28-35.
- Hunt, L., Reynolds, S., Brown, T., Hadley, S., Downton, J. and Chopra, S., 2010. Quantitative estimate of fracture density variations in the Nordegg with azimuthal AVO and curvature: a case study. *The Leading Edge*, 29: 1122-1137.
- Jadoon, I.A., Bhatti, K.M., Siddiqui, F.I., Jadoon, S.K., Gilani, S.R. and Afzal, M., 2005. Subsurface fracture analysis in carbonate reservoirs: Kohat/Potwar plateau, north Pakistan. In *SPE/PAPG Ann. Techn. Conf.*, OnePetro.
- Jaumé, S.C. and Lillie, R.J., 1988. Mechanics of the Salt Range - Potwar Plateau, Pakistan - A fold-and-thrust belt underlain by evaporites. *Tectonics*, 7: 57-71.
- Joshi, R.M. and Singh, K.H., 2020. Carbonate reservoirs: recent large to giant carbonate discoveries around the world and how they are shaping the carbonate reservoir landscape. In: *Petrophysics and Rock Physics of Carbonate Reservoirs*. Springer, Singapore: 3-14.
- Lisle, R.J., 1994. Detection of zones of abnormal strains in structures using Gaussian curvature analysis. *AAPG Bull.*, 78: 1811-1819.
- Marfurt, K.J., Kirilin, R.L., Farmer, S.H. and Bahorich, M.S., 1998. 3D seismic attributes using a running window semblance-based algorithm. *Geophysics*, 63: 1150-65.
- Murray, G.H. 1968. Quantitative fracture study-sanish pool, Mckenzie County, North Dakota. *AAPG Bull.*, 52: 57-65.
- Nasseri, A., Mohammadzadeh, M.J. and Raeisi, H.T., 2015. Fracture enhancement based on artificial ants and fuzzy c-means clustering (FCMC) in Dezful Embayment of Iran. *J. Geophys. Engineer.*, 12: 227-241.
- Olson, J.E., Laubach, S.E. and Lander, R.H., 2009. Natural fracture characterization in tight gas sandstones: Integrating mechanics and diagenesis. *AAPG Bull.*, 93: 1535-1549.

- Pedersen, S., Randen, T. and Sonneland, L., 2001. Automatic extraction of fault surfaces from three-dimensional seismic data. Expanded Abstr., 71st Ann. Internat. SEG Mtg., San Antonio: 551-554.
- Pennock, E.S., Lillie, R.J., Zaman, A.S.H. and Yousaf, M. 1989. Structural interpretation of seismic reflection data from eastern Salt Range and Potwar Plateau, Pakistan. AAPG Bull., 73: 841-857.
- Randen, T., Monsen, E., Signer, C., Abrahamsen, A., Hansen, J.O., Sæter, T. and Schlaf, J., 2000. Three-dimensional texture attributes for seismic data analysis. Expanded Abstr., 70th Ann. Internat. SEG Mtg., Calgary, AB: 668-671.
- Roberts, A., 2001. Curvature attributes and their application to 3D interpreted horizons. First Break, 19: 85-100.
- Roehl, P.O. and Choquette, P.W., 1985. Perspectives on world-class carbonate petroleum reservoirs. AAPG Bull., 69: 148.
- Spence, G.H., Redfern, J., Aguilera, R., Bevan, T.G., Cosgrove, J.W., Couples, G.D. and Daniel, J.-M., 2015. Advances in the Study of Fractured Reservoirs. Geological Society of London.
- Wandrey, C.J., Law, B.E. and Shah, H.A., 2004. Patala-Nammal composite total petroleum system, Kohat-Potwar Geologic Province, Pakistan. US Geological Survey, Reston: 1-18.
- Wennberg, O.P., Casini, G., Jonoud, S. and Peacock, D.C.P., 2016. The characteristics of open fractures in carbonate reservoirs and their impact on fluid flow: A discussion. Petrol. Geosci., 22: 91-104.
- Yasin, Q., Ding, Y., Baklouti, S., Boateng, C.D., Du, Q. and Golsanami, N., 2021. An integrated fracture parameter prediction and characterization method in deeply buried carbonate reservoirs based on deep neural network. J. Petrol. Sci. Engineer.: 109346.